First Results From Sleuth: The Palomar Planet Finder

Francis T. O'Donovan, David Charbonneau, Lewis Kotredes

California Institute of Technology, M/C 105-24, 1200 E California Blvd, Pasadena, CA 91125

ftod, dc, ltk@astro.caltech.edu

Summary

We discuss preliminary results from our first search campaign for transiting planets performed using Sleuth, an automated 10 cm telescope with a 6 degree square field of view. We monitored a field in Hercules for 40 clear nights between UT 2003 May 10 and July 01. We obtained an rms precision (per 15-min average) over the entire data set of better than 1% on the brightest 2026 stars, and better than 1.5% on the brightest 3865 stars. We identified no strong candidates in the Hercules field. We conducted a blind test of our ability to recover transiting systems by injecting signals into our data and measuring the recovery rate as a function of transit depth and orbital period. We find that about 85% of transit signals with a depth of 0.02 mag are recovered. However, only 50% of transit signals with a depth of 0.01 mag were recovered. We expect that the number of stars for which we can search for transiting planets will increase substantially for our current field in Andromeda, due to the lower Galactic latitude of the field and increased precision resulting from hardware improvements.

Sleuth conducts its automated transit search from a clamshell enclosure at Palomar Observatory in Southern California.

Sleuth as observed by Snoop, the Palomar All-Sky Camera. Mars is visible at the bottom of the image, and the Moon is rising to the left. Current and archived images and movies of the Palomar night sky are available at snoop.palomar.caltech.edu.

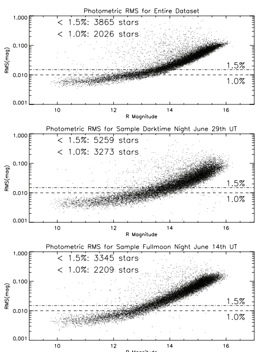

Figure 1: The calculated rms as a function of R magnitude for the 10,000 brightest stars in our Hercules field for three subsets of data: (upper panel) all observations; (center panel) observations from a single night during new moon; (lower panel) observations from a single night during full moon. The numbers of stars with rms below 1.0% and 1.5% for each dataset are shown.

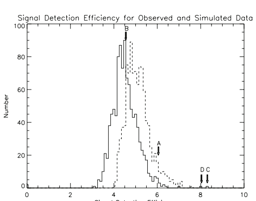

Figure 2: The solid line shows the histogram of derived Signal Detection Efficiency (SDE) values (an estimate of our confidence in a given signal) for the best-fit transit signal for each of the 1000 brightest stars. We also replaced each timeseries of the 1000 brightest stars by Gaussian-distributed data with the same mean and variance. The histogram of derived SDE values for this simulated data set is plotted as the dashed line. The phased time series for two stars with large SDE values (indicated on the plot) are shown in Figures 6 & 7. We also inserted transits into the data and attempted to recover these: phased light curves of two such recovered systems are shown in Figure 3, and the resulting SDE values are indicated on the plot for the actual data (A) and the simulated Gaussian data (B).

Acquisition and Analysis of Sleuth Observations

Sleuth, located at Palomar Observatory in Southern California, is the third transit-search telescope in our network which comprises STARE (PI: T. Brown, located in Tenerife), and PSST (PI: E. Dunham, located in northern Arizona). Sleuth is an f/2.8 lens with a 10 cm aperture that images a 6 degree square field of view onto a 2048 x 2048 back-illuminated CCD camera. Sleuth conducts nightly observations with the SDSS r' filter, but also gathers color images in g', i', & z' during new moon. Sleuth automatically adjusts the focus for changes in temperature and filter. A separate f/6.3 lens feeds the guide camera. The automated observations, including operation of the clamshell enclosure, are controlled by a workstation running Linux. In the event of threatening weather, the on-site night assistant for the 200" telescope can close the system remotely, and an observatory weather station provides additional protection. At dawn, the night's data are automatically compressed and sent by ftp to our workstation at Caltech.

From May 10 to July 01 2003, we monitored approximately 10,000 stars ($9 < R < 16$) in a field in Hercules. Figure 1 shows the calculated rms error in our photometry. We applied the STARE photometry code (written by T. Brown [HAO/NCAR] and with adaptations by G. Mandushev [Lowell Obs.]) to calibrate the images and to obtain light curves of the stars.

We then used Mandushev's transit search program (based on the box-fitting algorithm of Kovacs, Zucker & Mazeh, A&A, 391, 369 [KZM]) to search these light curves for transits with periods ranging from 1.5 to 7.5 days. This program assigned a Signal Detection Efficiency (SDE - see KZM) to the star, based on the significance of the transit detection. Figure 2 shows a histogram of the SDEs of the thousand brightest stars in the Hercules field, and compares it with the SDEs of a thousand model stars with a Gaussian noise distribution of the same mean and variance as the original timeseries.

We also tested the transit search code by inserting simulated transits into our photometric data and attempting to recover these data - an example of such an injected transit is shown in Figure 3. The recovery rate of these transits is shown in Figure 4, and the SDEs of the transits computed by the code are plotted in Figure 5.

Future Work

The Hercules data were often subject to large night-to-night pixel offsets, due to a firmware error in our guider. We have now repaired this problem. Whereas the typical offsets in Hercules were 20 pixels, in our current field (in Andromeda), these offsets rarely exceed 3 pixels, and guiding within a single night is often good to 1 pixel.

A by-product of our observations will be the detection of hundreds of variable and eclipsing stars per field. Example light curves of such systems are shown in Figures 6, 7, & 8. We intend to compile a catalog of detected variable stars.

A dominant concern for any transit survey is the rejection of false positives, i.e. systems containing an eclipsing binary, which mimic the photometric light curve of a transiting planet. One way to rule out such systems is by multi-epoch spectroscopic follow-up, but such work is resource-intensive. An alternative is to conduct higher-angular-resolution, multicolor photometry of transit candidates. To this end, we are currently buildling Sherlock, an automated follow-up telescope for wide-field transit searches, which will be located in the same enclosure as Sleuth. Please see our Sherlock poster (first author L. Kotredes).

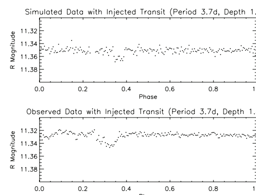

Figure 3: As a test of our ability to recover transit signals, we injected transits of varying period and depth into the data, as well as into simulated data, where each star's timeseries was replaced by Gaussian distributed data with the same mean and variance. The recovered 1.4%-deep transits for a 3.7 day period for two such stars are shown for the simulated data (upper panel) and actual data (lower panel). The SDE values for these recoveries are shown in Figure 2.

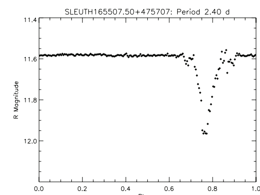

Figure 6: Light curve for a grazing-incidence eclipsing binary system, phased to the detected period of 2.40 days. The SDE value for this system is shown in Figure 2.

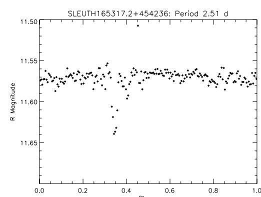

Figure 7: Phased time series of a low-amplitude eclipsing system with a period of 2.51 days. The SDE for this object is indicated on Figure 2.

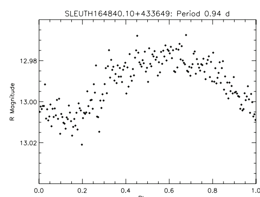

Figure 8: Phased light curve for one of the numerous low-amplitude variable stars that we detected. The period is 0.94 days.

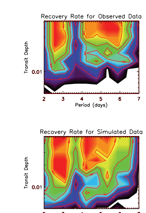

Figure 4: The recovered percentage of injected transit signals for the thousand brightest stars in our sample (upper panel) and in our simulated data (lower panel), as a function of period and transit depth. The grid is coarsely sampled (10 x 10), due to computation limitations. Red areas indicate a nearly complete recovery rate, whereas white areas indicate that virtually no such signals were recovered. Intermediate values of roughly 20% & 50% are shown as blue and green contours, respectively.

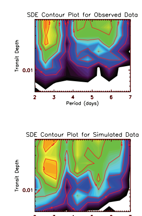

Figure 5: Contours indicating the average SDE values for the recovered transits of a given period and depth for the observed data (upper panel) and the simulated data (lower panel). These values can be compared with the histograms in Figure 2.